Hindawi
International Journal of Polymer Science
Volume 2021, Article ID 7491679, 10 pages
https://doi.org/10.1155/2021/7491679

Research Article

Study on Compaction and Machinability of Silicon Nitride (Si3N4) Reinforced Copper Alloy Composite through P/M Route

T. Sathish,[1] **V. Mohanavel**,[2] **Alagar Karthick**,[3] **M. Arunkumar**,[4] **M. Ravichandran**,[5] **and S. Rajkumar**[6]

[1]*Department of Mechanical Engineering, Saveetha School of Engineering, SIMATS, 602105 Chennai, Tamil Nadu, India*
[2]*Centre for Materials Engineering and Regenerative Medicine, Bharath Institute of Higher Education and Research, Chennai, 600073 Tamil Nadu, India*
[3]*Department of Electrical and Electronics Engineering, KPR Institute of Engineering and Technology, Coimbatore, 641407 Tamil Nadu, India*
[4]*Department of Agriculture Engineering, Sri Shakthi Institute of Engineering and Technology, Coimbatore, 641062 Tamil Nadu, India*
[5]*Department of Mechanical Engineering, K.Ramakrishnan College of Engineering, Trichy 621112, Tamil Nadu, India*
[6]*Department of Mechanical Engineering, Faculty of Manufacturing, Institute of Technology, Hawassa University, Ethiopia*

Correspondence should be addressed to S. Rajkumar; rajkumar@hu.edu.et

Received 11 April 2021; Accepted 23 June 2021; Published 8 July 2021

Academic Editor: Ching Hao Lee

Nowadays, most of the products are used in the electrical and electronics field, and copper alloy is playing a significant role such as Springs for relay contacts and switchgear, Rotor bars, and Busbars. In this work, the copper alloys consider as base alloy, and the reinforced factor of silicon nitride (Si_3N_4) is processed of reinforcement as 3 wt. %, 6 wt. %, 9 wt. %, 12 wt. % Si_3N_4 through powder metallurgy performance. The ball mill process is used for this work to obtain an enhanced homogeneous mixture of both base material as well as reinforced particles. Using a hydraulic press, the blended powders are compacted with applying 3 kN and 10 min period for obtained good strength of green compact specimens. Further, the green compacted specimens are sintered, and the sintered billets are machined in the conventional lathes with different cutting speeds 50 m/min, 100 m/min, and 150 m/min; feed rate of 0.1 mm/rev (fixed); and depth of cut of 0.5 mm, 0.8 mm, 1 mm, 1.2 mm, 1.4 mm, and 1.6 mm. Cutting speed and depth of cut to find the composites' cutting force is ingenious. A wear test also can be conducted to find the wear resistance of the reinforced particles of the copper alloy material.

1. Introduction

With the development of new materials, the composite functions majorly with low mass ratio to potency ratios and enhanced properties. The standard composite is metal matrix composites. These are high strength, magnificent wear, and corrosion behavior and have high mechanical properties. The powder metallurgy route is the best way to fabricate all parts in simple compacting and heating metal powders [1, 2]. The machining of MMCs is complex due to superior hardness value, the tool wear is more, and the surface finish attains poor condition. The Aluminium Matrix Composites (AMCs) are simple ones to replacing MMCs by their nature of strength and lightweight, and these alloys are suitable for structural work, aerospace, and automotive sectors. The polymer composite is also used for the fabrication of automotive components to improve their strength. Polymer composites possess high strength and lightweight [3, 4].

Powder metallurgy is a versatile process of producing composites within a short period. The preparation of powders, blending of powders, and the compaction process are indirect effects of the composites' machinability process [5–7]. The sintering process increases the strength of the composites and affects the cutting force of the tool. Based

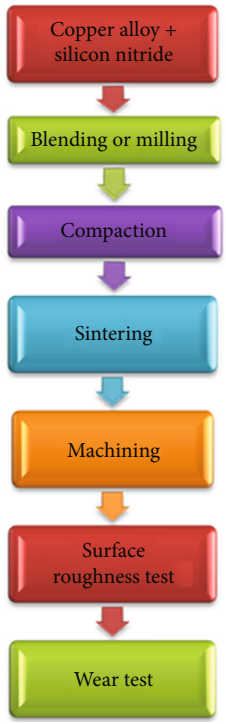

Figure 1: Flowchart of the proposed study.

Table 1: Chemical composition of copper alloy.

Elements	Cu	Al	Mg	Mn	Si	Cr
Weight%	98.05	0.42	0.29	0.47	0.24	0.24

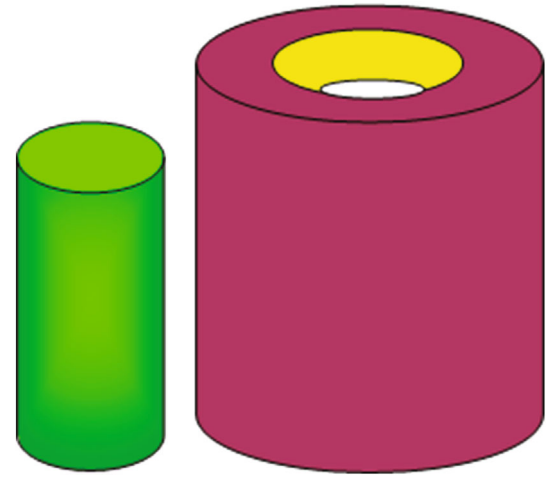

Figure 2: Punch and die for the compaction.

Table 2: Sintering process sequence.

Sintering process	Temperature		Time
	Starting	Ending	
Heating process	35°C	400°C	50 min
Soaking process	400°C	400°C	40 min
Heating process	400°C	500°C	40 min
Soaking process	500°C	500°C	40 min
Heating process	500°C	600°C	40 min
Soaking process	600°C	600°C	50 min
Allowed to cooling in the furnace	600°C	35°C	—

on the material, the tool selection was an important one [8–11]. The compaction process in the P/M tightens the loose powder effectively by applying different compaction pressure and selects the proper die and punch. There are forced particles mixed into the base material due to the blending or milling process [12]. The effects of reinforcement in the composite reflect in the tool wear. Most of the tool materials are affected by machining speed and feed rate [13]. Numerous methodologies are used to manufacture aluminum composites and other composites. Most composites are prepared by powder metallurgy and stir casting approach; most researchers develop their composites through these techniques. The stir casting method is termed liquid state processing which the base material has to be melted well and stir continually with the addition of solid reinforcement particles. This process considers the time for carrying out stirring action to increase the composites' strength. After stirring, action followed the solidification process to improve the solid strength of the composites. Stir casting examination offered the low-cost, simple in-process control of liquid state molten material. But some of the limitations are caused by the stir casting process, such as difficulty obtaining homogeneous mixture and possibly producing porosity in the composites. High temperature leads to poor wetting and a chance to form a reaction between the base and reinforced particles. The researchers undertake all these considerations. The powder metallurgy process is used to prepare the composites with multiple reinforcement particles in a single process. It can be provided the enhanced mechanical strength as well as tribological properties of the hybrid composites.

Some researchers carried out the PM method, mixing Al_2O_3into the aluminum and copper powders; the excellent mechanical strength was found. When developing composites, ductility is considered a factor in improving the composites' strength [14]. In some literature, the silicon nitride (Si_3N_4) was used to reinforce into the alloys the composites' ductility has to be obtained excellently and improve fracture toughness. Silicon nitride is one of the hard ceramic particles. It possesses high fracture toughness. Few of the literature only considered the silicon nitride ceramic particles into the aluminum alloy composites. The copper alloys have exceptional corrosion resistance. It has widely used in mechanical areas such as the joining of rivets and screws. Usually, copper alloys are called metal alloys. In that alloy, copper has a chief element of the copper alloys.

In general, copper and its alloys possess high electrical and thermal properties, continually better corrosion resistance, and superior ductility in nature for use in various engineering applications [15]. These alloys' limitations are low tensile strength and minimum wear resistance; this limitation needs enforcement in the silicon nitride ceramic particles to solve the limitations. Silicon nitride reinforced particles have

(a) (b)

Figure 3: Compacted billets (a) before sintering and (b) after sintering.

high thermal, mechanical, and wear properties to reinforce the base material to enhance material strength. Si_3N_4 ceramic particles offered better compressive strength than any composites since they possess superior compressive strength and yield strength [16]. Copper alloys and silicon carbide hard particles improve the microhardness of the composite materials. The wear resistance of the composites also increases hugely. Using silicon nitride, the homogeneous mixture was obtained in the P/M process route. The ball milling process was enhanced the mixture strength, such as base alloys and silicon nitride hard particles. The sintering process lifted the strength of the composites through melting. Both the base alloys and silicon nitride was moved to red hot condition and obtained uniform distribution [17]. This study planned to prepare the copper alloys with reinforced silicon nitride by implementing powder metallurgy practice. The main objectives of this work were mentioned, such as to find the machinability characteristics and wear property of the copper alloy composites prepared by the powder metallurgy practice with different input parameters. The sintered composites are machined by using of conventional lathe machine with different machining parameters such as cutting speed, feed rate, and depth of cut. The result of cutting force is measured by the influence of cutting speed and depth of cut. The machinability study is focusing on machining of the copper nozzle and bushes, a wear study aimed to prevent the wear in the commutator in an electric motor.

2. Materials and Method

This experiment considers the copper alloys to reinforce silicon nitrite with a different weight percentage of composition [18]. The experiment plan was illustrated in Figure 1, and the material selection is the initial phase of this work. The material is chosen for this work as copper alloys and silicon nitride. Copper alloys are primarily used in electrical items such as motor winding and electrical wire. The powder metallurgy process highly blends both the materials; continually, the compaction process is carried out. Further, green compaction is sintered and extruded. Finally, the machinability, surface roughness, and wear test were conducted. Table 1 presented the constituent elements of copper alloys generally X-ray fluorescence (XRF) technique was used to measure the material's elemental composition. The atomized powder particles of copper alloys and the different weight percentages of the silicon nitride were mixed into the ball mill with a uniform speed of 400rpm, with a few steel balls being induced the powders'.

Table 3: Machining parameters.

Tool bit material	High-speed steel (HSS)
Cutting speed in m/min	50, 100,150
Feed rate in mm/rev	0.1 (fixed)
Depth of cut in mm	0.5, 0.8, 1, 1.2,1.4,1.6
Percentage of reinforcement % wt. Si_3N_4	3, 6, 9,12

Uniform mixing in the ball mill, the blending operation carried out 1 hour 30 minutes [19]. The mixed powder particles are filled in the cylindrical die cavity. The powders are pressed by the application of pressure, the punch and die of the experiment were illustrated in Figure 2. The hydraulic press complied under the specifications of 10 kN capacity and the ram's stroke length as 300 mm. The 3 kN pressure was applied while compaction with maintaining the pressure for 10 min [20]. The sintering sequence is presented in Table 2, and the Green compact billets are further sintered by using of sintering process in the furnace. The billets are placed inside the furnace in the order of reinforcement percentage to collect the billets after sintering [21]. Initially, the starting temperature of the sintering process at 35°C was applied, continually heating up to 400°C after reaching 400°C to maintain the same temperature for 40 min. Further heating 400°C to 500°C, the furnace reached 500°C to maintain the same temperature at the time of 40 min [22–24]. In the last attempt of heating 500°C to 600°C, the furnace reached the temperature of 600°C and maintains the same temperature for 40 min. After that, they allowed reducing

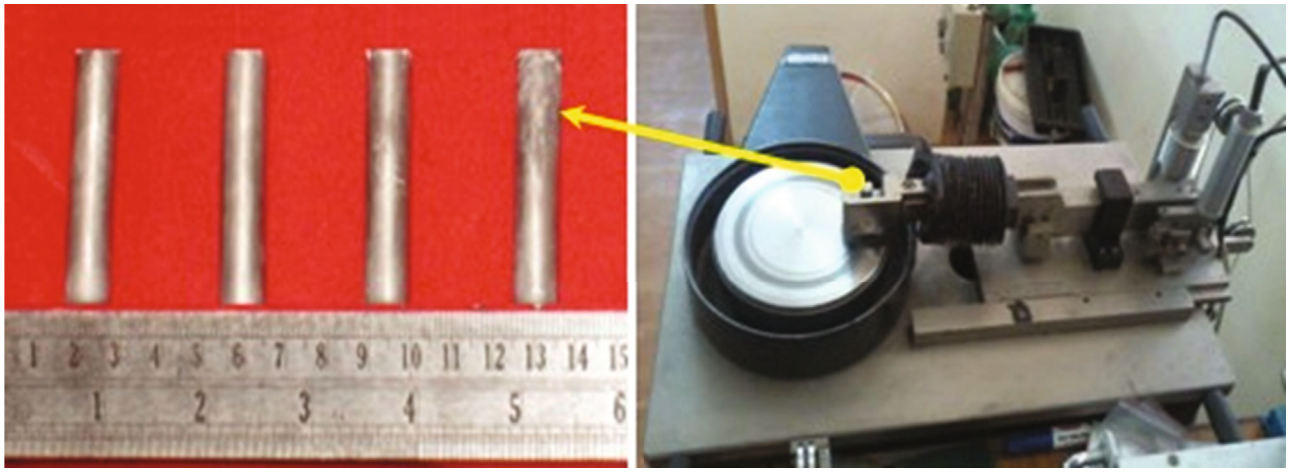

Figure 4: DUCOM dry sliding wear tester with specimens.

Table 4: Summary of machining parameters with the result of surface roughness.

S. no	Feed rate in (mm/rev)	Cutting speed in (m/min)	Depth of cut (mm)	Surface roughness values in microns			
				3 wt. %	6 wt. %	9 wt. %	!2 wt. %
1	0.1	50	0.5	0.58	1.52	2.08	2.65
2			0.8	0.75	1.58	2.09	2.68
3			1.0	0.92	1.68	2.10	2.74
4			1.2	0.67	1.54	1.07	2.69
5			1.4	0.69	1.63	2.15	2.72
6			1.6	0.83	1.57	2.17	2.78
7		100	0.5	0.95	1.68	2.23	2.8
8			0.8	1.02	1.72	2.37	2.81
9			1.0	1.34	1.86	2.29	2.80
10			1.2	1.25	1.67	2.34	2.76
11			1.4	1.34	1.73	2.42	2.84
12			1.6	1.21	1.81	2.45	2.83
13		150	0.5	1.32	1.92	2.53	2.94
14			0.8	1.42	1.96	2.57	2.97
15			1.0	1.28	1.89	2.74	3.01
16			1.2	1.34	1.94	2.64	3.11
17			1.4	1.47	2.01	2.58	3.12
18			1.6	1.39	2.05	2.62	3.16

the temperature of 600°C to 35°C. The compact green billets before sintering and after sintering are shown in Figure 3. The soaking process is essential to modifying the composite billets' microstructure [25–28].

The conventional machining process was carried out in the lathe machine with different speeds, constant feed rates, and depth of cut. The HMT lathe machine was used for machining the composites with the aid of a high-speed steel tool material. The Mitutoyo surface roughness tester is measured by the machined components' surface roughness [29–31]. The cutting force was measured by using of lathe tool dynamometer made by National instruments effectively; the machining parameters of this investigation are presented in Table 3.Wear test experiments under the influence of 3.0 kgf of applied, sliding velocity of 2 m/s, the sliding distance of 1500 m, and the wear track diameter of 120 mm [32–34]. The disc rotational speed is maintained at 160 rpm with a

Table 5: Cutting force summary (cutting speed 50 m/min).

S. no	Depth of cut (mm)	Cutting force (kgf)			
		3 wt. %	6 wt. %	9 wt. %	12 wt. %
1	0.5	2.34	2.89	3.01	3.76
2	0.8	4.56	5.32	4.56	6.37
3	1.0	6.75	7.24	7.34	8.28
4	1.2	8.24	9.15	10.45	10.72
5	1.4	10.23	12.34	12.78	14.89
6	1.6	12.74	13.24	14.23	16.76

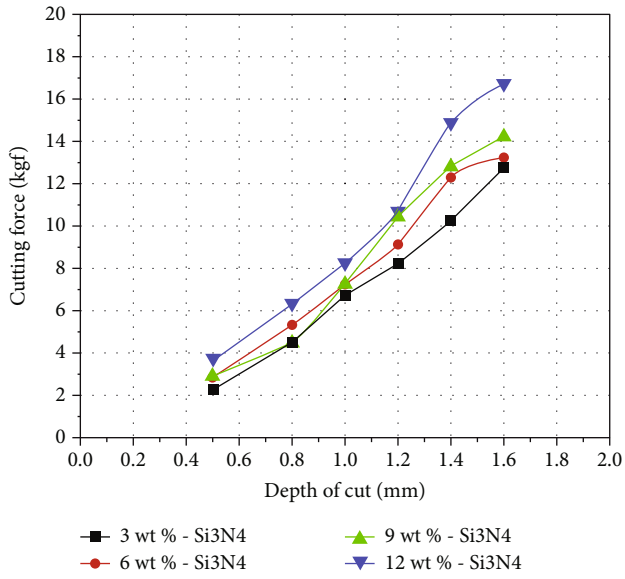

Figure 5: Depth of cut vs. cutting force (cutting speed 50 m/min).

Table 6: Cutting force summary (cutting speed 100 m/min).

S. no	Depth of cut (mm)	Cutting force (kgf)			
		3 wt. %	6 wt. %	9 wt. %	12 wt. %
1	0.5	3.45	3.84	3.67	3.76
2	0.8	6.24	5.23	6.24	7.36
3	1.0	7.23	9.15	10.21	1.24
4	1.2	9.45	12.12	11.54	12.76
5	1.4	12.62	14.67	16.92	15.43
6	1.6	14.67	18.23	19.84	17.98

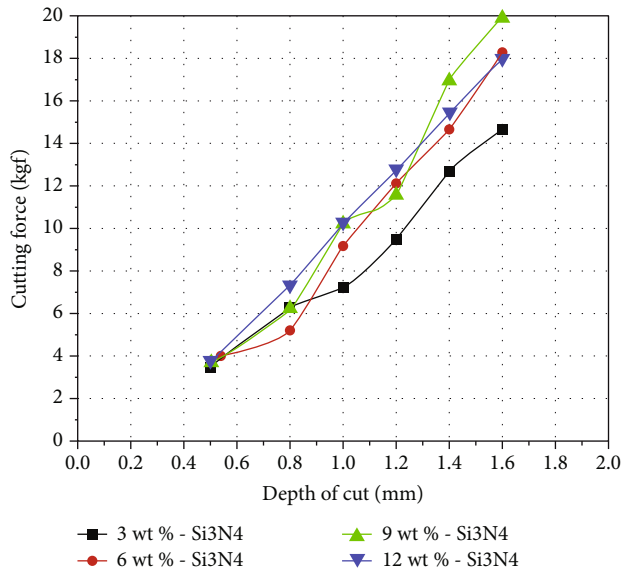

Figure 6: Depth of cut vs. cutting force (cutting speed 100 m/min).

time of 25 minutes. The dry sliding wear test specimens and apparatus of the DUCOM machine are effectively utilized for this research, as shown in Figure 4.

Table 7: Cutting force summary (cutting speed 150 m/min).

S. no	Depth of cut (mm)	Cutting force (kgf)			
		3 wt. %	6 wt. %	9 wt. %	12 wt. %
1	0.5	1.89	2.37	3.01	2.56
2	0.8	3.65	4.62	4.52	5.34
3	1.0	7.23	8.34	8.24	9.37
4	1.2	8.24	11.24	10.34	12.76
5	1.4	10.29	13.47	14.78	13.27
6	1.6	13.64	17.23	16.34	15.49

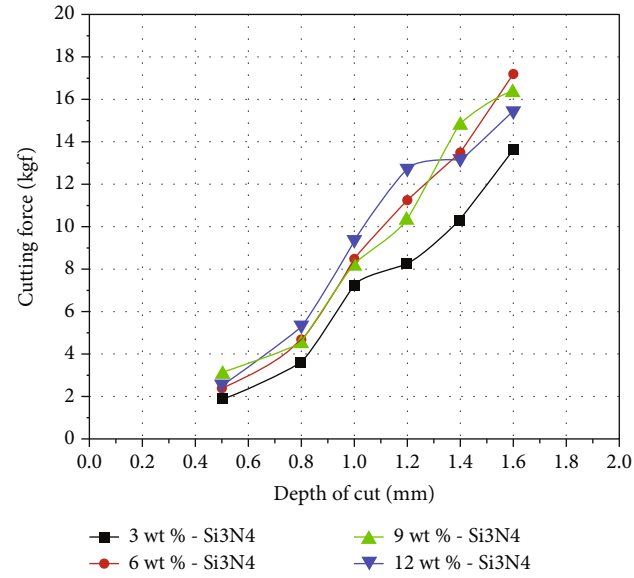

Figure 7: Depth of cut vs. cutting force (cutting speed 150 m/min).

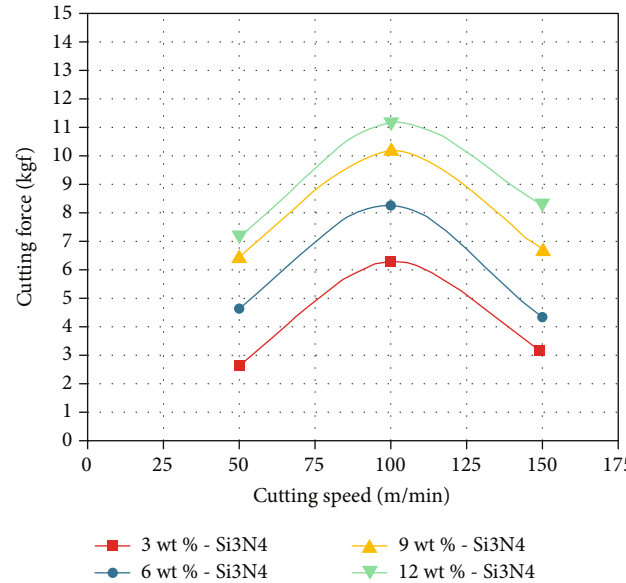

Figure 8: Cutting speed vs. cutting force (depth of cut 0.5 mm).

Different reinforcement percentages of wear test specimens are prepared under 10 mm diameter and 40 mm length with power tool cutting. Specimens are cleaned well before

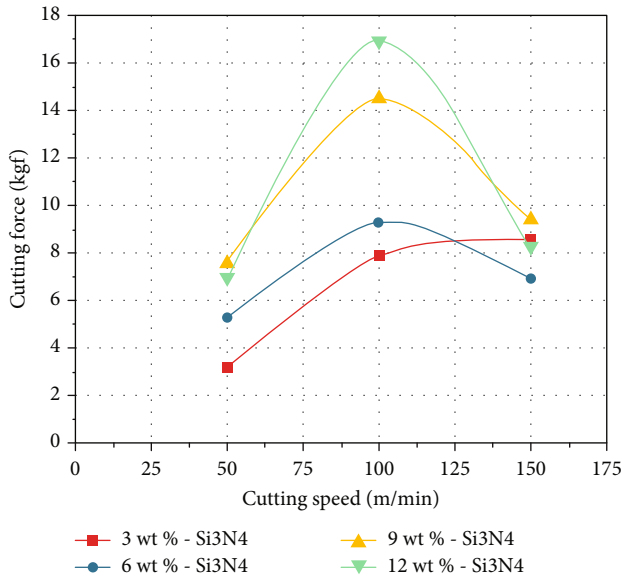

Figure 9: Cutting speed vs. cutting force (depth of cut 0.8 mm).

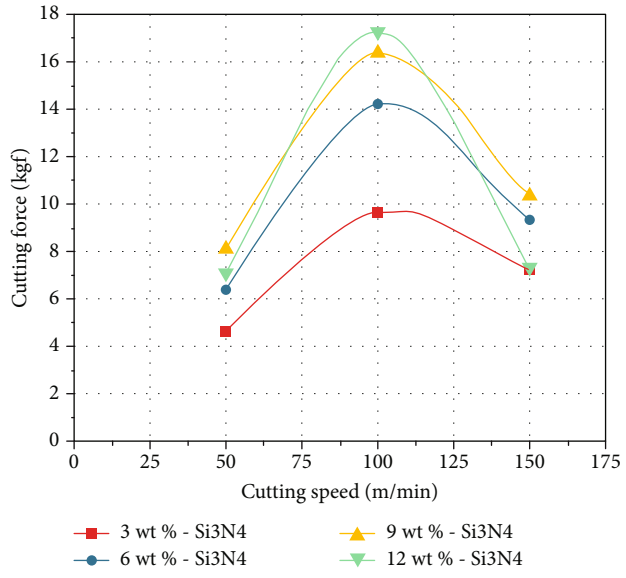

Figure 10: Cutting speed vs. cutting force (depth of cut1.0 mm).

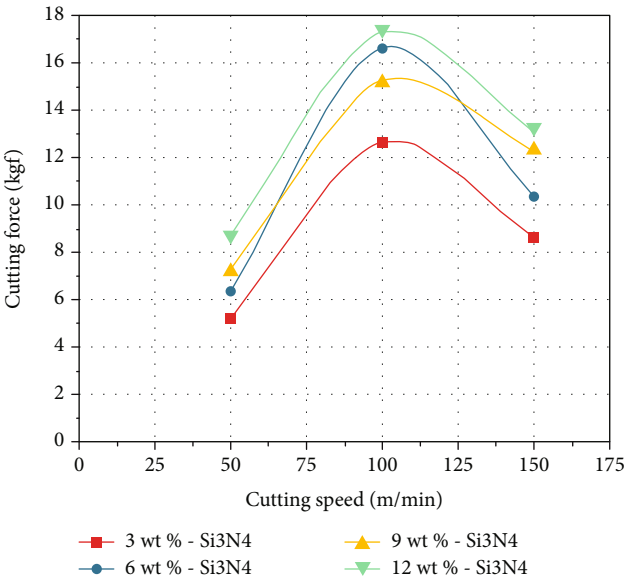

Figure 11: Cutting speed vs. cutting force (depth of cut 1.2 mm).

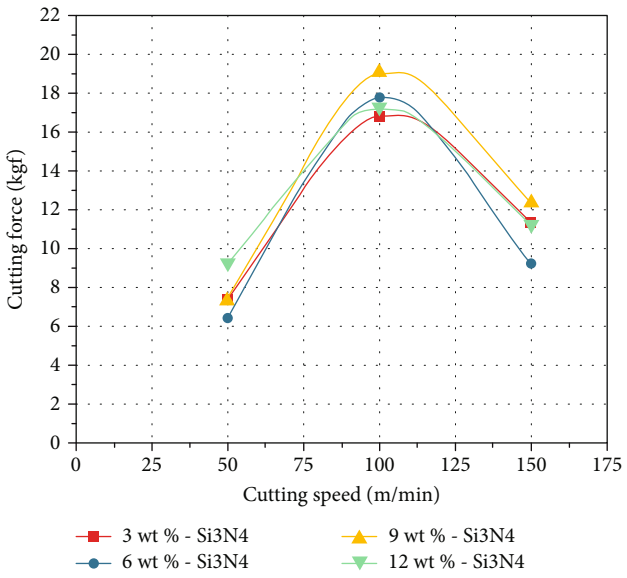

Figure 12: Cutting speed vs. cutting force (depth of cut 1.4 mm).

carried out the wear test. All the samples are prepared and wear-tested as per the American Society of Testing Materials (ASTM G99) standard procedure [35–37].

3. Results and Discussion

Table 4 clearly illustrated the influence of machining parameters and the result of surface roughness value. The surface roughness values are increased by increasing of reinforcement percentage of silicon nitride. The cutting speed and the reinforcement percentage were directly influenced to maximize the surface roughness value. The maximum surface roughness value was obtained as 3.16 microns by reinforcement of 12 wt. %, cutting speed of 150 m/min, depth of cut 1.6 mm, and the constant federate 0.1 mm/rev. The minimum surface roughness value obtained is 0.58 microns. Increasing reinforcement increases the tool wear and increases the surface roughness value. Increasing reinforcement increases the strength of the composites in terms of toughness and hardness, leading to affect the tool edges. Further, it can be reflected by poor surface finish.

3.1. Effects of Cutting Speed. The Cutting force summary of influencing Cutting speed 50 m/min is presented. The cutting force increases by increasing the depth of the cut and increasing reinforcement percentage Table 5. The maximum cutting force attained was 16.76 kgf at reinforcement of 12 wt. % of silicon nitride with the depth of cut as 1.6 mm. The minimum cutting force is 2.34 kgf by influencing 3 wt. % of reinforcement and the 0.5 depth of cut as shown in Figure 5.

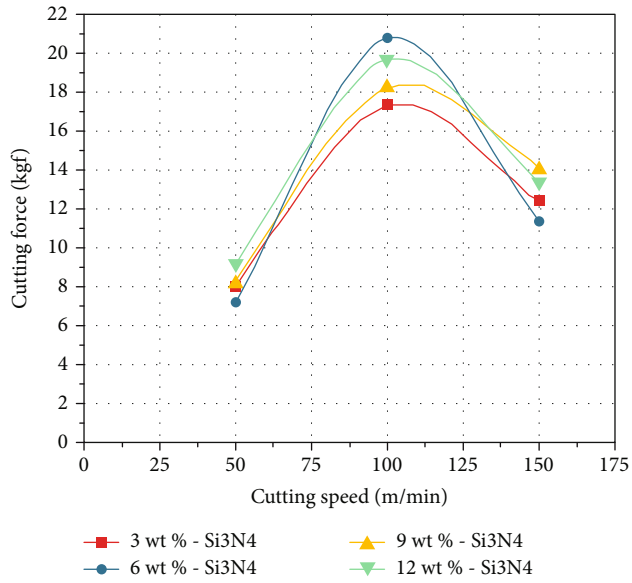

Figure 13: Cutting speed vs. cutting force (depth of cut 1.6 mm).

Table 8: Summary of wear test.

S. no	Load (*N*)	Sliding velocity (m/s)	Sliding distance (m)	Track diameter (mm)	Wear time (min)	Wear results Reinforcement %	Wear (microns)	Frictional force
1	30	2	1500	120	25	3	211	1.2
2						6	182	1.4
3						9	174	1.5
4						12	188	1.4

The cutting force analysis by influencing cutting speed 100 m/min is illustrated. The cutting force constantly increases with increasing depth of cut and increasing reinforcement weight percentage. Maximum cutting force obtained as 17.98 kgf by the reinforcement of 12 wt. % with the depth of cut as 1.6 mm in Table 6. The low cutting force was 3.45 kgf by persuading 3 wt. % of reinforcement and the 0.5 depth of cut, as shown in Figure 6.

In the cutting force study, by influencing cutting speed 150 m/min, the cutting force regularly increases with increasing cut and increasing reinforcement weight percentage in Table 7. The maximum value of cutting force was 15.49 kgf by their enforcement of 12%, with the depth of cut as 1.6 mm. The 1.89 kgf cutting force was attained by inducing 3 wt. % of reinforcement and the 0.5 depth of cut, as shown in Figure 7. Compared to cutting speed 100 m/min, the cutting force value decreased by applying 100 m/min.

3.2. Effects of Depth of Cut. The cutting force's effects were analyzed by variation of cut depth shown in Figures 8–13. The minimum cutting force obtained as 2.58 kgf with 50 m/min influence was shown in Figure 9. The maximum cutting force was obtained as 20.86 kgf with 12 wt. % reinforcement and the 100 m/min cutting speed, as shown in Figure 13, which presented the wear results. The constant values of applied load (30 N), sliding velocity (2 m/s), track diameter (120 mm), and wear time (25 min) were continued to all four specimens with different reinforcement percentages. Increasing reinforcement particles (Si_3N_4) conversely reduced the wear. Further increasing of reinforcement percentage can be turned to increases the wear rate Table 8.

The wear graph was presented in Figure 14 effectively; the maximum wear was 211 microns using 3 wt. % of Si_3N_4. Using a testing time of 25 minutes, the average frictional force was illustrated as 1.0. During the wear process, the temperature would be continually maintained as 287°C. For increasing reinforcement, reduction reduces the wear finally reached the maximum reinforcement it caused to increase wear. Minimum wear was obtained as 174 microns with 9 wt. % of reinforcement. High reinforcement percentage was induced lower mixing level. Further, it can be the origin of high weight loss. These reinforcement composites offered better wear resistance even in increasing temperature and the higher speed of the wear test.

4. Conclusion

The powder metallurgy technique carried out the machinability study of copper alloys with silicon nitride. The different machining parameters as cutting speed, feed rate, depth

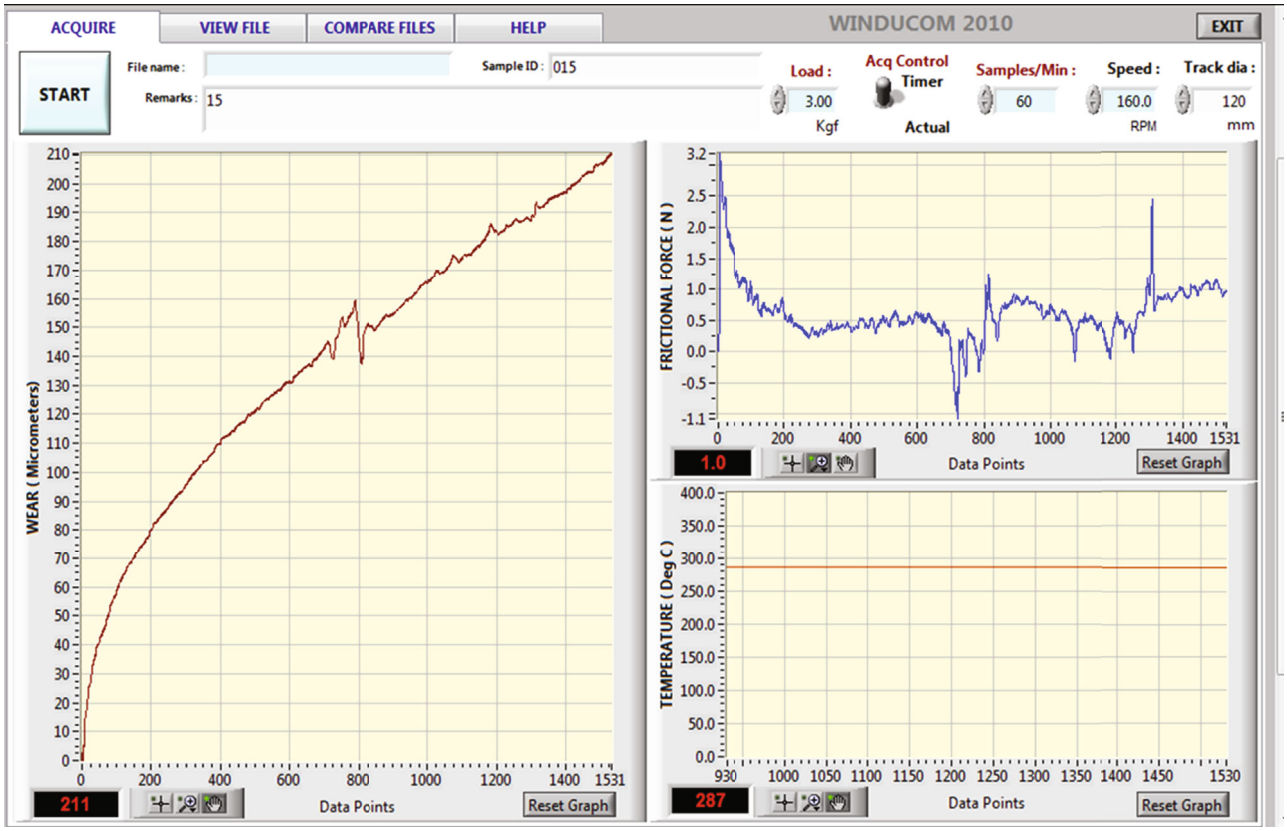

Figure 14: Wear test output in graphical view.

of cut, and reinforcement percentage were executed to measure the composite's surface roughness and cutting force effectively. The result of this investigation was presented as follows:

(i) The cutting speed and the reinforcement percentage were directly influenced to maximize the surface roughness value from the analysis. The maximum surface roughness value obtained was 3.16 microns by reinforcement of 12 wt. %, cutting speed of 150 m/min, depth of cut 1.6 mm, and the constant feed rate 0.1 mm/rev. The minimum surface roughness value obtained is 0.58 microns. Increasing reinforcement increases the tool wear and increases the surface roughness value

The maximum cutting force attained is 16.76 kgf at reinforcement of 12 wt. % of silicon nitride with the depth of cut as 1.6 mm. The minimum cutting force is 2.34 kgf by influencing 3 wt. % of reinforcement and the 0.5 depth. The cutting speed is 100 m/min, and the maximum cutting force is obtained as kgf by the reinforcement of 12 wt. % with the cut's depth as 1.6 mm. The low cutting force was 3.45 kgf by persuading 3 wt. % of reinforcement and 0.5 depth. For the cutting speed of 150 m/min, the maximum value of cutting force was 15.49 kgf by their enforcement of 12 wt. % with the depth of cut as1.6 mm. The 1.89 kgf cutting force was attained by inducing 3 wt. % of reinforcement and the 0.5 depth of cut.

(ii) From the analysis, the maximum cutting force obtained was 20.86 kgf with the influence of 12 wt. % reinforcement and the 100 m/min cutting speed. The minimum cutting force obtained was 2.58 kgf with an influence of 50 m/min

(iii) From the wear test, the minimum wear was obtained as 174 microns with 9 wt. % of reinforcement. Maximum wear was obtained as 211 microns by reinforcement of 3 wt. % of Si_3N_4. The increasing tendency of reinforcement reduces the wear and finally reached the 9 wt. % to 12 wt. % of reinforcement it caused to increase wear

Data Availability

The data used to support the findings of this study are included within the article.

Conflicts of Interest

The authors declare that there is no conflict of interest regarding the publication of this article.

References

[1] M. Kilic, D. Ozyurek, and T. Tuncay, "Dry sliding wear behaviour and microstructure of the W–Ni–Fe and W–Ni–Cu heavy alloys produced by powder metallurgy technique," *Powder*

Metallurgy and Metal Ceramics, vol. 55, no. 1-2, pp. 54–63, 2016.

[2] S. Chand and P. Chandrasekhar, "Influence of B4C/BN on solid particle erosion of Al6061 metal matrix hybrid composites fabricated through powder metallurgy technique," *Ceramics International*, vol. 46, no. 11, pp. 17621–17630, 2020.

[3] D. Rahmadiawan, A. Hairul, N. Nasruddin, and Z. Fuadi, "Stability, viscosity, and tribology properties of polyol ester oil-based biolubricant filled with TEMPO-oxidized bacterial cellulose nanofiber," *International Journal of Polymer Science*, vol. 2021, Article ID 5536047, 9 pages, 2021.

[4] Y. Zeleke and G. K. Rotich, "Design and development of false ceiling board using polyvinyl acetate (PVAc) composite reinforced with false banana fibres and filled with sawdust," *International Journal of Polymer Science*, vol. 2021, Article ID 5542329, 10 pages, 2021.

[5] H. Alihosseini, K. Dehghani, and J. Kamali, "Microstructure characterization, mechanical properties, compressibility and sintering behavior of Al-B4C nanocomposite powders," *Advanced Powder Technology*, vol. 28, no. 9, pp. 2126–2134, 2017.

[6] S. L. G. Petroni, "PM compaction equations applied for the modelling of titanium hydride powders compressibility data," *Powder Metallurgy*, vol. 63, no. 1, pp. 35–42, 2020.

[7] F. Güner, Ö. N. Cora, and H. Sofuoğlu, "Numerical modeling of cold powder compaction using multi particle and continuum media approaches," *Powder Technology*, vol. 271, pp. 238–247, 2015.

[8] N. Sharma and K. Kumar, "Mechanical characteristics and bioactivity of porous Ni50-xTi50Cux (x =0, 5and 10) prepared by P/M," *Materials Science*, vol. 34, no. 8, pp. 934–944, 2018.

[9] A. Saboori, C. Novara, M. Pavese, C. Badini, F. Giorgis, and P. Fino, "An investigation on the sinterability and the compaction behavior of aluminum/graphene nanoplatelets (GNPs) prepared by powder metallurgy," *Journal of Materials Engineering and Performance*, vol. 26, no. 3, pp. 993–999, 2017.

[10] P. Verma, R. Saha, and D. Chaira, "Waste steel scrap to nanostructured powder and superior compact through powdermetallurgy: powdergeneration, processing and characterization," *Powder Technology*, vol. 326, pp. 159–167, 2018.

[11] A. Saker, M. G. Cares-Pacheco, P. Marchal, and V. Falk, "Powders flowability assessment in granular compaction: what about the consistency of Hausner ratio?," *Powder Technology*, vol. 354, pp. 52–63, 2019.

[12] A. Fathy, E.-K. Omyma, and M. M. M. Mohammed, "Effect of iron addition on microstructure, mechanical and magnetic properties of Al-matrix composite produced by powder metallurgy route," *Transactions of Nonferrous Metals Society of China*, vol. 25, no. 1, pp. 46–53, 2015.

[13] M. A. Sohag, P. Gupta, N. Kondal, D. Kumar, N. Singh, and A. Jamwal, "Effect of ceramic reinforcement on the mi- crostructural, mechanical and tribological behavior of Al-Cu alloy metal matrix composite," *Materials Today: Proceedings*, vol. 21, pp. 1407–1411, 2020.

[14] Y. Tian, Z. Dou, L. Niu, and T. Zhang, "Effect of nanoboron carbide particles on properties of copper-matrix/graphite composite materials," *Materials Research*, vol. 6, no. 9, pp. 950–957, 2019.

[15] M. Zhou, S. Huang, L. Yu, W. Liu, and S. Yan, "Investigation on compaction densification behaviors of multicomponent mixed metal powders to manufacture silver-based filler metal sheets," *Arabian Journal for Science and Engineering*, vol. 44, no. 2, pp. 1321–1335, 2019.

[16] W. Chen, J. Wang, S. Wang, P. Chen, and J. Cheng, "On the processing properties and friction behaviours during compaction of powder mixtures," *Materials Science and Technology*, vol. 36, pp. 1057–1064, 2020.

[17] C. Ayyappadas, A. Muthuchamy, A. R. Annamalai, and D. K. Agrawal, "An investigation on the effect of sintering mode on various properties of copper-graphene metal matrix composite," *Advanced Powder Technology*, vol. 28, no. 7, pp. 1760–1768, 2017.

[18] A. H. Jaafar and H. Al-Ethari, "Optimization of machining nickel aluminum bronze matrix composite prepared by powder metallurgy," in *International Conference on Advances in Sustainable Engineering and Applications (ICASEA)*, pp. 255–260, Wasit - Kut, Iraq, 2018.

[19] D. Sujit, R. Behera, G. Majumdar, B. Oraon, and G. Sutradhar, "An experimental investigation on the machinability of powder formed silicon carbide particle reinforced aluminium metal matrix composites," *International Journal of Scientific & Engineering Research*, vol. 2, no. 7, pp. 2229–5518, 2011.

[20] M. B. N. Shaikh, S. Arif, and M. A. Siddiqui, "Fabrication and characterization of aluminium hybrid composites reinforced with fly ash and silicon carbide through powder metallurgy," *Materials Research Express*, vol. 5, no. 4, 2018.

[21] K. Halil, O. İsmail, D. Sibel, and Ç. Ramazan, "Wear and mechanical properties of Al6061/SiC/B4C hybrid composites produced with powder metallurgy," *Journal of Materials Research and Technology*, vol. 8, no. 6, pp. 5348–5361, 2019.

[22] P. V. Badiger, V. Desai, M. R. Ramesh, B. K. Prajwala, and K. Raveendra, "Cutting forces, surface roughness and tool wear quality assessment using ANN and PSO approach during machining of MDN431 with TiN/AlN-coated cutting tool," *Arabian Journal for Science and Engineering*, vol. 44, no. 9, pp. 7465–7477, 2019.

[23] M. O. Shabani, A. Baghani, A. Khorram, and F. Heydari, "Evaluation of fracture mechanisms in Al-Si metal matrix nanocomposites produced by three methods of gravity sand casting, squeeze casting and compo casting in semi-solid state," *Silicon*, vol. 12, no. 12, pp. 2977–2987, 2020.

[24] R. Harichandran and N. Selvakumar, "Microstructure and mechanical characterization of (B4C+ h-BN)/Al hybrid nanocomposites processed by ultrasound assisted casting," *International Journal of Mechanical Sciences*, vol. 144, pp. 814–826, 2018.

[25] M. S. Kumar, M. Vanmathi, and G. Sakthivel, "SiC reinforcement in the synthesis and characterization of A356/AL2O3/-Sic/Gr reinforced composite-paving a way for the next generation of aircraft applications," *Silicon*, pp. 1–18, 2020.

[26] K. A. Ali, V. Mohanavel, M. Ravichandran, S. A. Vendan, T. Sathish, and A. Karthick, "Microstructure and mechanical properties of friction stir welded SiC/TiB 2 reinforced aluminum hybrid composites," *Silicon*, pp. 1–11, 2021.

[27] A. Nirala and A. Upadhyaya, "Experimental characterization and sintering behavior in mixed atmosphere (N 2 and H 2) of Fe 3 P-added ferritic stainless steel (434L)," *Journal of Materials Engineering and Performance*, vol. 29, no. 5, pp. 2926–2935, 2020.

[28] R. K. Behera, S. C. Panigrahi, B. P. Samal, and P. K. Parida, "Mechanical properties and micro-structural study of sintered aluminium metal matrix composites by P/M technique,"

Journal of Modern Manufacturing Systems and Technology, vol. 3, no. 2, pp. 89–97, 2019.

[29] V. Kavimani, B. Stalin, P. M. Gopal, M. Ravichandran, A. Karthick, and M. Bharani, "Application of r-GO-MMT hybrid nanofillers for improving strength and flame retardancy of epoxy/glass fibre composites," *Advances in Polymer Technology*, vol. 2021, 9 pages, 2021.

[30] R. Bhagat, "Advanced aluminium powder metallurgy alloy and composites," in *ASM Hand Book*, vol. 7, pp. 840–858, ASM International, Cleveland OH, 2018.

[31] N. Sharma, T. Raj, and K. K. Jangra, "Microstructural evaluation of NiTi-powder, steatite, and steel balls after different milling conditions," *Materials and Manufacturing Processes*, vol. 31, no. 5, pp. 628–632, 2016.

[32] S. A. Daniel, M. Sakthivel, P. M. Gopal, and S. Sudhagar, "Study on tribological behaviour of Al/SiC/MoS2 hybrid metal matrix composites in high temperature environmental condition," *Silicon*, vol. 10, no. 5, pp. 2129–2139, 2018.

[33] I. Gunes, T. Uygunoglu, and M. Erdogan, "Effect of sintering duration on some properties of pure magnesium," *Powder Metallurgy and Metal Ceramics*, vol. 54, no. 3-4, pp. 156–165, 2015.

[34] N. Radhika, J. Sasikumar, and R. Jojith, "Effect of grain modifier on mechanical and tribological properties of Al-Si alloy and composite," *Silicon*, vol. 13, no. 3, pp. 841–855, 2021.

[35] N. Raj and N. Radhika, "Tribological characteristics of LM13/Si3N4/Gr hybrid composite at elevated temperature," *Silicon*, vol. 11, no. 2, pp. 947–960, 2019.

[36] M. I. Haq and A. Anand, "Dry sliding friction and wear behavior of AA7075-Si3N4 composite," *Silicon*, vol. 10, no. 5, pp. 1819–1829, 2018.

[37] P. V. Badiger, V. Desai, M. R. Ramesh, B. K. Prajwala, and K. Raveendra, "Effect of cutting parameters on tool wear, cutting force and surface roughness in machining of MDN431 alloy using Al and Fe coated tools," *Materials Research Express*, vol. 6, no. 1, pp. 89–97, 2018.